https://doi.org/10.31436/iiumej.v27i3.3409

Comparison of Fatigue Crack Growth Models for Predicting Residual Life

MUHAMMAD HUSNAIN MOHD NOH[1], MOHD AKRAMIN MOHD ROMLAY[1*], MOHD SHAMIL SHAARI[1], AKIYUKI TAKAHASHI[2]

[1]Faculty of Mechanical & Automotive Engineering Technology, Universiti Malaysia Pahang Al-Sultan Abdullah, 26600 Pekan, Pahang Darul Makmur, Malaysia
[2]Tokyo University of Science, 2641 Yamazaki, Noda, Chiba 278-8510, Japan

**Corresponding author: akramin@umpsa.edu.my*

(Received: 19 August 2024; Accepted: 10 February 2026; Published online: 11 September 2026)

ABSTRACT: Fatigue is one of the most critical failure mechanisms in structural materials. Accurate prediction of fatigue crack growth and residual fatigue life is essential to ensure structural safety and reliability during design and service-life assessment. This study aims to predict the residual fatigue life of a four-point bending specimen under fatigue loading conditions using the S-version finite element model (S-version FEM). Four fatigue crack growth models are implemented within the S-version FEM framework, namely Paris' Law, Frost and Pook, Walker, and Huang Moan models, to simulate crack propagation and estimate residual fatigue life. Experimental data from Al7075-T6 are used for validation purposes. The results indicate that the Frost and Pook model achieves an error below 20%, demonstrating acceptable engineering accuracy. In contrast, the Paris' Law, Walker, and Huang Moan models show significantly higher deviations from the experimental results. Overall, the Frost and Pook model exhibits the best agreement with the experimental findings and provides improved predictive capability compared to the other empirical models, confirming the effectiveness of the proposed S-version FEM approach for fatigue crack growth and residual fatigue life prediction in four-point bending structures.

ABSTRAK: Retak-lesu merupakan salah satu mekanisme kegagalan paling kritikal dalam bahan struktur. Ramalan yang tepat terhadap pertumbuhan retak-lesu dan baki jangka hayat adalah penting bagi memastikan keselamatan dan kebolehpercayaan struktur dalam reka bentuk serta penilaian hayat perkhidmatan. Kajian ini bertujuan bagi meramalkan baki jangka hayat retak-lesu spesimen lenturan empat titik menggunakan model unsur terhingga S-version (S-version FEM) di bawah beban keletihan. Empat model pertumbuhan retak-lesu dijalankan dalam rangka kerja S-version FEM, iaitu Hukum Paris, Frost dan Pook, Walker, dan Huang Moan bagi mensimulasikan penyebaran retak serta menganggar baki jangka hayat retak-lesu. Data eksperimen daripada Al7075-T6 digunakan untuk tujuan pengesahan model. Keputusan menunjukkan bahawa model Frost dan Pook memberikan ralat kurang daripada 20%, sekaligus menunjukkan ketepatan kejuruteraan yang boleh diterima. Sebaliknya, model Hukum Paris, Walker, dan Huang Moan menunjukkan sisihan lebih tinggi berbanding keputusan eksperimen. Secara keseluruhan, model Frost dan Pook menunjukkan kesepadanan terbaik dengan keputusan eksperimen serta memberikan keupayaan ramalan yang lebih baik berbanding model empirik yang lain, sekaligus mengesahkan keberkesanan pendekatan S-version FEM yang dicadangkan dalam meramal pertumbuhan retak-lesu dan baki jangka hayat bagi struktur lenturan empat titik.

KEYWORDS: *Residual life; S-version finite element model; Fatigue Crack Growth Models*

1. INTRODUCTION

Typically, more than 90% of engineering component failures are attributed to fatigue. The primary objective of fatigue crack growth (FCG) analysis is to identify the parameters governing crack initiation and propagation under cyclic loading conditions. Therefore, understanding fatigue crack growth behavior is essential because it significantly influences structural integrity and material performance. Fatigue crack growth problems are complex to simulate because of the nonlinear nature of crack initiation and propagation mechanisms. Although several numerical methods, including the hybrid method, the Extended Finite Element Method (XFEM), and the conventional Finite Element Method (FEM), have been widely applied, each presents notable limitations. The hybrid method is associated with high computational cost; XFEM requires complex formulation and implementation; while conventional FEM struggles to accurately capture evolving crack paths without remeshing.

In fracture mechanics, fatigue life estimation has been extensively developed based on crack propagation analysis. One of the most important parameters in this field is the stress intensity factor (SIF), which characterizes the stress field near the crack tip and governs crack growth behavior [1]. However, accurately predicting fatigue crack growth in complex geometries remains challenging. Conventional FEM is widely used for such analyses, but it requires continuous remeshing as cracks propagate, making it computationally expensive and inefficient, particularly for three-dimensional problems [2].

To overcome these limitations, the S-version FEM has been developed. This method significantly reduces remeshing requirements and enables efficient simulation of complex crack propagation paths [2]. The S-version FEM is commonly integrated with linear elastic fracture mechanics (LEFM) for fatigue crack growth and residual life prediction. In LEFM, the stress concentration near the crack tip, expressed through the SIF, is a key parameter in describing crack propagation behavior.

Furthermore, fatigue crack growth rates are typically predicted using empirical crack growth laws combined with LEFM principles [3]. FEM is widely applied to evaluate fracture mechanics parameters such as SIF and energy release rate, which quantify crack driving forces and stress concentration at the crack tip [4]. Fatigue is defined as the progressive and localized structural degradation of materials subjected to repeated cyclic loading [5]. Therefore, accurate prediction of FCG is essential for estimating the remaining useful life of engineering components and remains a major focus in both academic and industrial research [6, 7].

The fatigue crack growth rate is commonly described using material constants and the SIF range, which govern crack propagation behavior [8]. Crack growth significantly reduces the fatigue life of engineering structures. From a fracture mechanics perspective, the energy release rate represents the rate of energy transformation during crack propagation. Numerical approaches such as the virtual crack closure technique (VCCT) [9], [10] and the J-integral method [11, 12] are widely implemented within FEM frameworks to evaluate the energy release rate. Both energy release rate and SIF are strongly correlated and widely used in fatigue analysis.

The VCCT determines the energy required to close a crack by multiplying nodal reaction forces with crack opening displacements [4]. Its advantages include computational simplicity and the ability to decompose energy release rates into mode I, mode II, and mode III components. VCCT has been successfully applied to various three-dimensional fracture mechanics problems [4, 13, 14].

FCG models are mathematical formulations used to predict crack propagation rates under cyclic loading conditions [3]. Common models include Paris' Law [15], the Wheeler model [16], the Forman model [17], the Walker model [18], the Frost & Pook model [19], and the modified Paris-Erdogan model [20], among others [21-23]. These models aim to describe crack growth behavior over loading cycles [20]. Although numerous models have been proposed, their comparative performance within advanced numerical frameworks remains insufficiently investigated.

Among these models, Paris' Law is one of the most widely used empirical formulations for predicting fatigue crack growth under cyclic loading. Paris, Gomez, and Anderson initially introduced the relationship in 1961, and Paris and Erdogan subsequently formalized it in 1963 [15]. It relates the fatigue crack growth rate, (da/dN), to the SIF range, (ΔK), using a power-law relationship and has been extensively validated and refined for various engineering materials [24]. However, the original Paris formulation is mainly applicable to the stable crack growth region under constant-amplitude loading and a fixed stress ratio. It does not explicitly account for stress-ratio effects, crack-growth thresholds, load-sequence interactions, or retardation caused by overloads. The Frost and Pook model provides an alternative formulation in which the fatigue crack growth rate is related to the square of the SIF range and the material's elastic properties [25]. This formulation introduces greater sensitivity to material behavior and can be useful when comparing crack growth characteristics across different materials. Nevertheless, the model does not explicitly incorporate load-history or load-interaction effects, which may limit its accuracy under complex variable-amplitude loading.

The Walker model extends Paris' Law by introducing the stress ratio (R) through an equivalent SIF range and a material-dependent exponent, allowing fatigue crack growth data obtained under different stress ratios to be unified into a single relationship and improving prediction accuracy when mean stress varies; however, it remains an empirical steady-state model and does not capture load-sequence effects such as overload-induced retardation or underload acceleration [26-28]. In contrast, the Huang Moan model provides a more comprehensive approach for variable-amplitude loading by combining an equivalent SIF (normalized to R = 0) with a modified Wheeler retardation concept [29, 30], while accounting for both stress-ratio effects and plastic zone size ahead of the crack tip, enabling it to describe key load-interaction phenomena such as crack growth retardation or temporary arrest after overloads and acceleration following underloads, and has been validated for materials such as aluminium alloys and structural steel under complex loading spectra; therefore, it is generally more suitable than the Paris, Frost & Pook, and Walker models for fatigue crack growth analyses involving variable-amplitude loading histories.

Fatigue crack initiation and propagation under cyclic loading are among the primary causes of structural failure. However, damage-tolerant structures are designed to sustain applied loads even in the presence of cracks or partial damage. Therefore, an understanding of fatigue crack growth laws is essential for damage-tolerant design and reliable fatigue life prediction [31]. This knowledge enables engineers to make informed decisions regarding structural design, maintenance scheduling, and performance optimization.

Fatigue and fracture failure modes significantly influence the integrity and reliability of metallic materials. Investigating these mechanisms is essential to ensure structural safety, enhance design reliability, and improve material performance across engineering applications. However, challenges such as multiscale material behavior, environmental effects, and experimental limitations make fatigue and fracture analysis highly complex. Therefore, advanced modeling techniques and accurate predictive approaches are essential for improving fatigue life estimation and structural integrity assessment.

2. METHODOLOGY

This study implements FCG models, namely Paris' Law, Frost & Pook, Walker, and Huang-Moan models, within the S-version FEM framework for fatigue life prediction. Integrating these models enables accurate simulation of crack propagation behavior and residual life estimation under cyclic loading conditions. Modern engineering structures require more precise and reliable assessment techniques due to increasing complexity in design, material properties, geometry, loading conditions, operating environments, manufacturing processes, and structural applications. Therefore, an advanced numerical approach is necessary to evaluate fatigue behavior using computational modeling. In this study, the VCCT is employed to compute fatigue crack growth parameters. VCCT is used to determine the energy required for crack propagation by evaluating nodal forces and crack opening displacements. Within the LEFM framework, the primary governing parameters for crack growth are the SIF and the energy release rate, which describe the stress state and energy driving crack propagation at the crack tip. The fatigue crack growth process is modeled using the computed SIF to predict crack extension per loading cycle. The number of cycles to failure is then determined by incrementally updating the crack length using the selected fatigue crack growth models until the critical crack size is reached.

2.1. S-version Finite Element Model (S-version FEM)

This section explains crack growth at the crack front within the S-version FEM framework. Important variables such as the SIF and energy release rate are employed to describe crack growth behavior in LEFM. The VCCT, which has been further developed to be compatible with the S-version FEM framework, is utilized to define the energy release rate [32]. The crack propagation direction at the crack front can be determined with the support of this extension [33]. Assuming that the faces of the finite element mesh are positioned orthogonally at the crack front, Fig. 1 illustrates the three-dimensional VCCT in its original configuration. As shown in Fig. 1, the nodal opening displacement P_i, where $(i = 1, 2, 3, 4, 5, 6)$, is measured near the crack front within the VCCT framework. The five nodes at the crack front boundary represent the opening displacement, v_i. S_1 and S_2 denote the areas of the finite element faces at the crack front segment.

As shown in Fig. 1, the displacement of the upper crack surface is represented by v_{iU}, while the displacement of the lower crack surface is denoted by v_{iL}. Therefore, the definition of the opening displacement v_i is given as follows [6]:

$$v_i = v_{iU} - v_{iL} \tag{1}$$

If the analysis incorporates a combination of global and local meshes, the displacement is calculated as the sum of the global and local displacement components for both the upper and lower crack surfaces. Accordingly, the displacement for both surfaces can be expressed as:

$$v_{iU} = v_{iU}^G - v_{iU}^L, v_{iL} = v_{iL}^G - v_{iL}^L \tag{2}$$

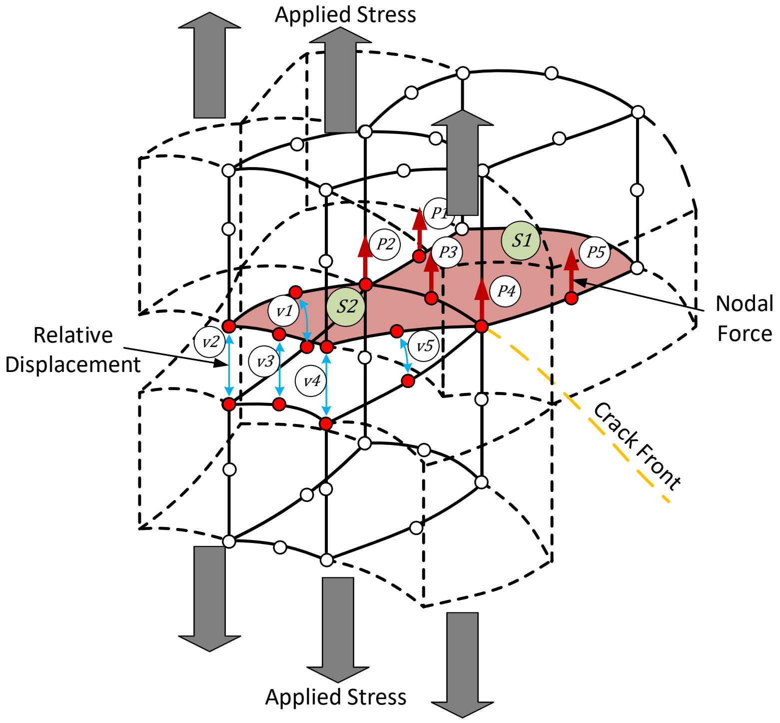

Figure 1. VCCT for local mesh at the crack front in three-dimensional analysis.

For this method, the opening displacement exists exclusively within the local mesh. In contrast, within the global region, the opening displacement is assumed to be zero. Therefore,

$$v_{iU}^{G} = -v_{iL}^{G} \tag{3}$$

Eqs. (1), (2), and (3) are combined to determine the cumulative opening displacement v_i at the nodes within the local region. The resulting expression for v_i is given as follows [34]:

$$v_i = \left(v_{iU}^{G} + v_{iU}^{L}\right) - \left(v_{iL}^{G} - v_{iL}^{L}\right) = v_{iU}^{L} - v_{iL}^{L} \tag{4}$$

The opening displacement around the crack front is computed first, followed by the energy release rate. Okada et al. [33] first introduced the energy release rate (start equation cap G) for the non-symmetrical configuration of finite element faces at the crack front. They proposed, as shown in Fig. 2, that the energy release, denoted by ΔG_I, is evaluated at the instant the crack front opens within the region S_1. This computation, which occurs during fracture propagation under Mode I failure, is expressed as follows:

$$\Delta G_I = \frac{1}{2}\int_{S_1} \sigma_{33}\,(r) v_3(\Delta - r) dS \tag{5}$$

The element configuration at the crack front is shown in Fig. 2, where r and Δ represent the element width and length, respectively, in directions perpendicular and parallel to the fracture front. Three fracture modes contribute to crack propagation: Mode I, Mode II, and Mode III. The cohesive stress, σ_{33}, within the crack front plane is indicated by the first subscript 3, which represents the face of the crack front in the vertical direction, and by the second subscript 3, which corresponds to the crack front coordinate system, x_1, x_2, and x_3, as seen in Fig. 2. The displacement v_i represents the crack opening displacement function in the Mode I direction. Broek [34] provides further details on stress and displacement at the crack face. The formulation for the cohesive stress and displacement function is given as follows:

$$\sigma_{33}(\bar{r}) = \frac{K_I}{\sqrt{2\pi\bar{r}}}, v_3(\bar{r}) = 4\sqrt{\frac{2\bar{r}}{\pi}}\frac{K_I}{E^*} \tag{6}$$

$E' = E/(1-v^2)$ represents the plane strain condition, while $E^* = E$ represents the plane stress condition. The Poisson's ratio and Young's modulus of the material are denoted by ν and E, respectively. The angle between the loading direction and the average crack front direction is denoted by θ, whereas $\bar{r}$ represents the distance from the crack front. By substituting the above expressions into Eq. (4), the stress and displacement fields can be expressed as follows:

$$\Delta G_I = \int_{\theta_1}^{\theta_2}\int_0^{\Delta} \frac{K_I}{\sqrt{2\pi r cos\emptyset}} 2\sqrt{\frac{2(\Delta - r)cos\emptyset}{\pi}}\frac{K_I}{E'}(R+r)\,dr\,d\theta \tag{7}$$

Therefore, the following equation can be used to represent Eq. (7), which describes the SIFs for the S_1 and S_2 regions, as illustrated in Fig. 2:

$$G_I = \frac{K_I^2}{E'} = \frac{1}{2\left[S_1 - \frac{1}{4}(S_1 - S_2)\right]}\sum_{i=1}^{5} v_i^3 P_i^3 \tag{8}$$

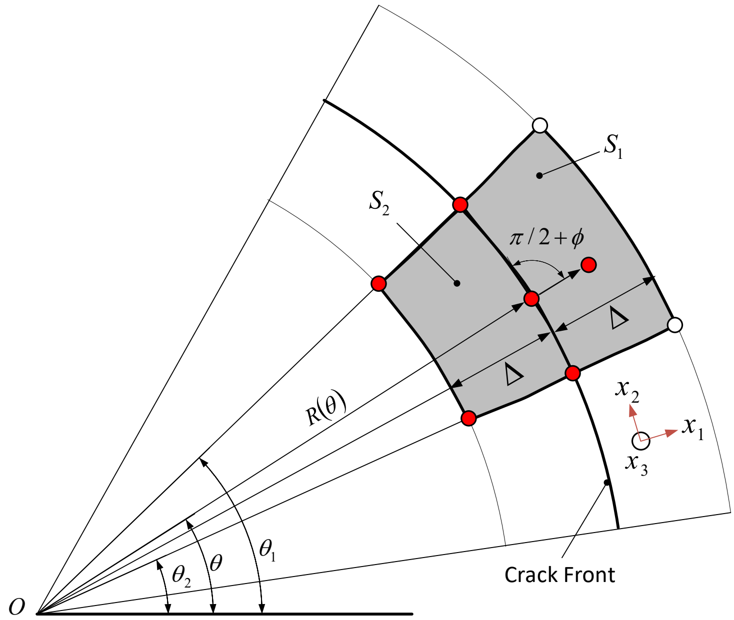

Figure 2. Element arrangement at the crack front of the material.

The energy release rate for the remaining failure modes is stated as follows:

$$G_{II} = \frac{K_{II}^2}{E^1} = \frac{1}{2\left[S_1 - \frac{1}{4}(S_1 - S_2)\right]}\sum_{i=1}^{5} v_i^1 P_i^1 \tag{9}$$

$$G_{III} = \frac{K_{III}^2}{2\mu} = \frac{1}{2\left[S_1 - \frac{1}{4}(S_1 - S_2)\right]}\sum_{i=1}^{5} v_i^2 P_i^2 \tag{10}$$

Here, the shear modulus is denoted by μ. In the energy release rate G, each component is represented by a subscript. The total energy release rate, G_{Total}, is obtained by summing G_I, G_{II}, and G_{III}. The conversion of the energy release rate to the SIF is possible, as shown in Eqs. (8), (9), and (10). For further details on the derivation of the element arrangement near the fracture front, refer to Okada et al. [33].

2.1.1. Paris Law Model

The Paris law, often expressed as a power law and originally proposed by Paris and Erdogan [15], is a well-known and straightforward method for predicting fatigue crack growth. This relationship provides the governing equation and marks one of the earliest applications of fracture mechanics to fatigue analysis.

$$\frac{da}{dN} = C_p(\Delta K)^n \tag{11}$$

where n is the slope and C_p is the intercept on the log–log plot of da/dN versus ΔK. Eq. (11) describes Region II of the fatigue crack growth rate curve, which exhibits a linear relationship on a log–log scale between da/dN and ΔK. The Paris law is simple to apply, requiring only two curve-fitting parameters that can be readily determined from experimental data. It is widely used in fatigue analysis, particularly when the experimental data exhibits a linear relationship in Region II.

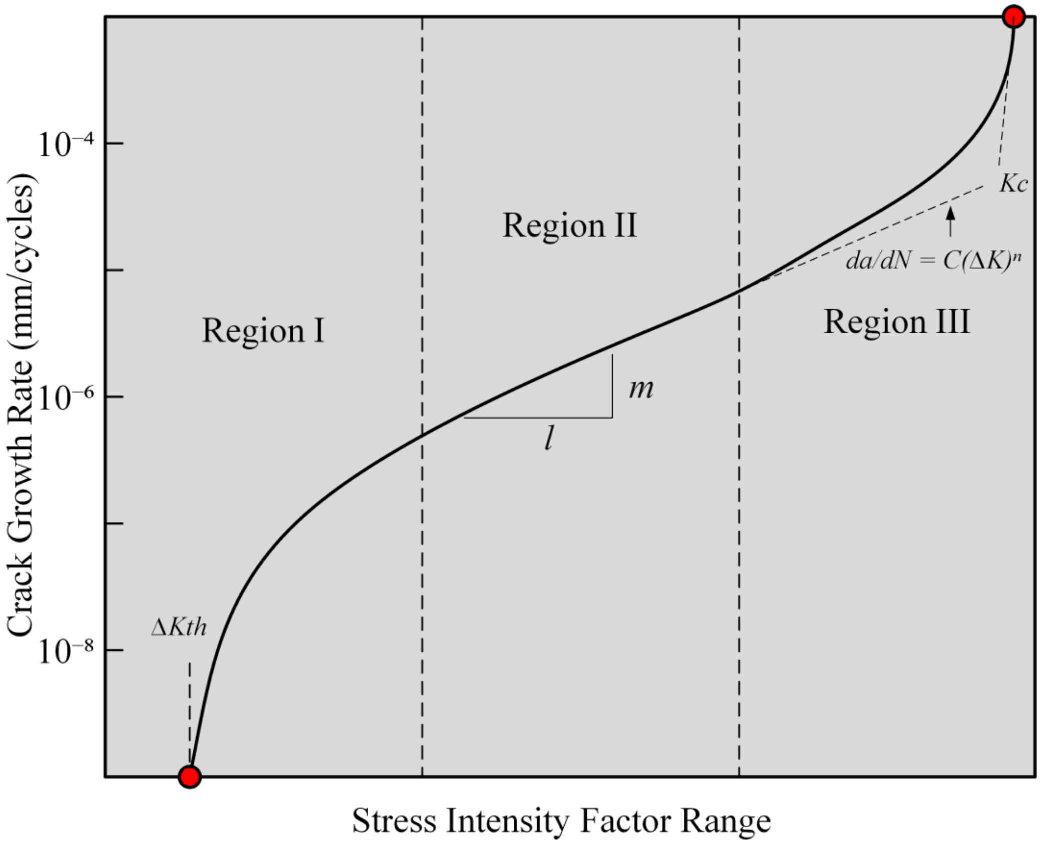

Figure 3. Typical da/dN versus ΔK curve $Log\ \Delta K$

The Paris law is limited to describing fatigue crack growth data in Region II (see Fig. 3). It cannot adequately characterize Regions I and III, where threshold behavior and rapid crack growth occur, respectively. Therefore, additional modeling approaches may be required depending on the nature of the analysis. Furthermore, the Paris law is material-dependent and does not account for the influence of stress ratio. For steels tested under different stress ratios, a family of parallel straight lines is typically obtained. This indicates that, while the value of C_p varies with stress ratio, the exponent n remains constant for a given material. As a result, ensure that fatigue crack growth data is applied using the appropriate stress ratio.

2.1.2. Frost & Pook Model

In 1971, Frost and Pook [19] developed an equation for fatigue crack growth that incorporates physical significance. According to their theory, cyclic loading causes cracks to propagate not through gradual structural damage, but because unloading reconfigures the crack tip after each cycle, which in turn forms striations [35]. Consequently, a simple model based on incremental crack growth per cycle can be related to the evolving crack tip geometry during opening and closure. The relationship is given as follows:

$$\frac{da}{dN} = \frac{9}{\pi}\left(\frac{\Delta K}{E}\right)^2 \text{ (plane stress)} \tag{12}$$

$$\frac{da}{dN} = \frac{7}{\pi}\left(\frac{\Delta K}{E}\right)^2 \text{ (plane strain)} \tag{13}$$

At crack growth rates of approximately 3×10^{-5}mm/cycle, a strong correlation was observed between experimental results plotted in terms of $\Delta K/E$ versus da/dN and the predictions of the plane stress formulation. However, at higher crack growth rates, the model tends to overestimate crack growth, while at lower rates it tends to underestimate it. Since ΔK is derived from the relationship between E' and the energy release rate G, the model implicitly incorporates the initial crack length and mean stress.

2.1.3. Huang Moan Model

Unlike the basic Paris law model, which does not explicitly incorporate stress ratio effects, the Huang Moan model accounts for the influence of stress ratio in the fatigue crack growth formulation [36]. The Huang and Moan model is mathematically expressed as:

$$\frac{da}{dN} = C_m\left(\mathrm{M}\Delta K_{eq}\right)^{n_m} \tag{14}$$

$$\text{where, } M = \begin{cases} (1-R)^{-1.2\beta} & (-5 \le R < 0) \\ (1-R)^{-\beta} & (0 \le R < 0.5) \\ (1.05 - 1.4R + 0.6R^2)^{-\beta} & (0.5 \le R < 1) \end{cases} \tag{15}$$

where C_m and n_m are material constants, M is a correction factor used to account for the mean stress effect over the range $-5 \le R < 1$, and ΔK_{eq} is the equivalent SIF range. The stress ratio range is divided into three intervals, and the correction factor M is used to shift fatigue crack growth curves at different stress ratios to the corresponding curve at $R = 0$. The parameter β is determined by fitting experimental fatigue crack growth data and is dependent on the material type [37].

2.1.4. Walker Model

The Walker model is commonly regarded as a traditional approach for estimating fatigue crack growth in different materials, especially in the stable crack propagation region [38]. The Walker model is expressed as:

$$\frac{da}{dN} = C_w\left[\frac{\Delta K_{eq}}{(1-R)^{1-\gamma}}\right]^{n_w} \tag{16}$$

The variables include a, which represents crack length, and N, which is the number of load cycles. C_w and n_w are material constants, while γ is the Walker coefficient specific to the material. ΔK denotes the SIF range, and R represents the stress ratio.

3. Results and Discussion

Fig. 4 shows the geometry of the four-point bending specimen subjected to fatigue loading. Based on the experimental configuration, the S-version FEM was applied to simulate the four-point bending setup. The model incorporates a semi-elliptical crack located at the center of the specimen [39, 40]. The initial crack length and depth were defined using experimental data from Akramin [41] were used to establish the initial crack's length and depth. The experimental setup was deliberately developed as a non-standard test rather than strictly adhering to ASTM standards. This approach better captures the behavior of real engineering structures under service-like conditions, where idealized ASTM loading and boundary assumptions may not fully represent actual structural responses. Although the ASTM four-point bending configuration serves as a useful benchmark for controlled laboratory testing, this study focuses on a more realistic scenario that reflects practical engineering applications. As a result, the non-standard experimental design improves the applicability of the findings to real-world engineering problems. Table 1 summarizes the material properties of Aluminum Alloy 7075-T6, which was selected for this study. This alloy was chosen due to its widespread use in older aircraft manufactured in the 1970s [20].

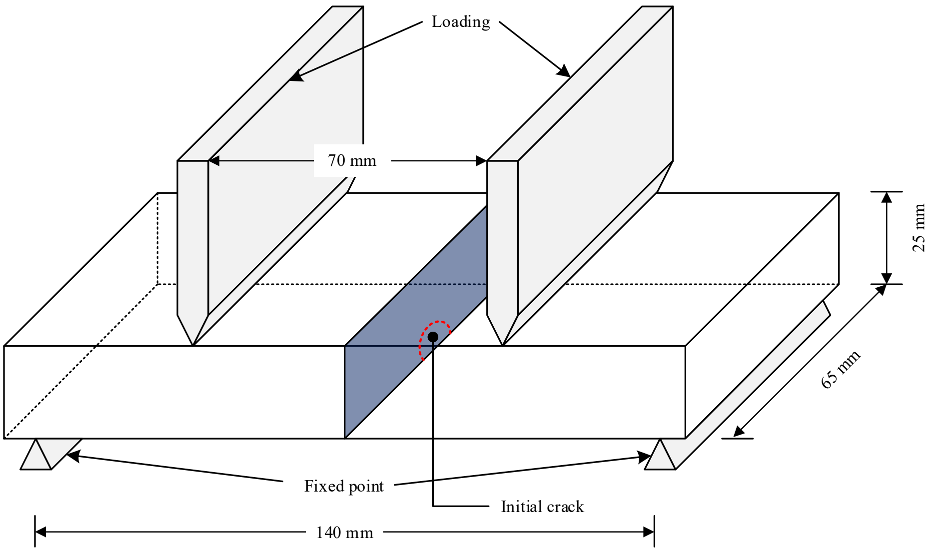

Figure 4. Geometry of four-point bending model.

The four-point bending model was subjected to fatigue loading with a stress ratio of 0.1, corresponding to a maximum load of 45 kN and a minimum load of 4.5 kN.

Table 1. Material properties of Aluminum Alloy 7075-T6

Variables	Values
Fracture toughness, K_{IC}	$29\ MPa.\sqrt{m}$
Young's modulus, E	$71.7\ GPa$
Tensile strength, Yield	$503\ MPa$
Poisson's ratio, ν	0.33
Fatigue power parameter, n	2.88
Paris coefficient, C	2.29×10^{-10}
The threshold value, K_{th}	$3.66 MPa.\sqrt{m}$

Fig. 5 compares fatigue-life predictions for the four-point bending model using Frost & Pook, Walker, Huang Moan, and Paris' Law approaches against the experimental data reported by Akramin et al. [41]. The results show a typical nonlinear crack-growth response, where the crack length increases gradually in early loading cycles, followed by an accelerated growth stage before catastrophic failure. The experimental results indicate an initial stable crack propagation stage, where the crack length increases slowly from approximately 4 mm to around 6 mm up to about 250×10^3 cycles. This is followed by a transition region where the crack growth rate begins to accelerate, leading to a rapid increase in crack length beyond approximately $350–380 \times 10^3$ cycles. Final failure occurs at approximately $450–460 \times 10^3$ cycles, where the crack length approaches 18–19 mm.

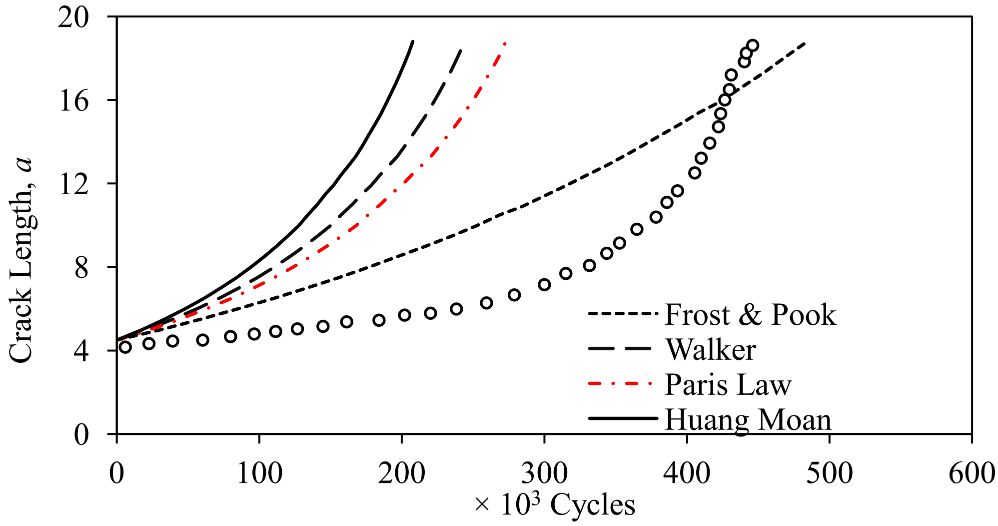

Figure 5. Comparison of experimental, Paris law model, Walker model, Huang Moan model and Frost & Pook model according to the four-point bending specimen's fatigue life prediction.

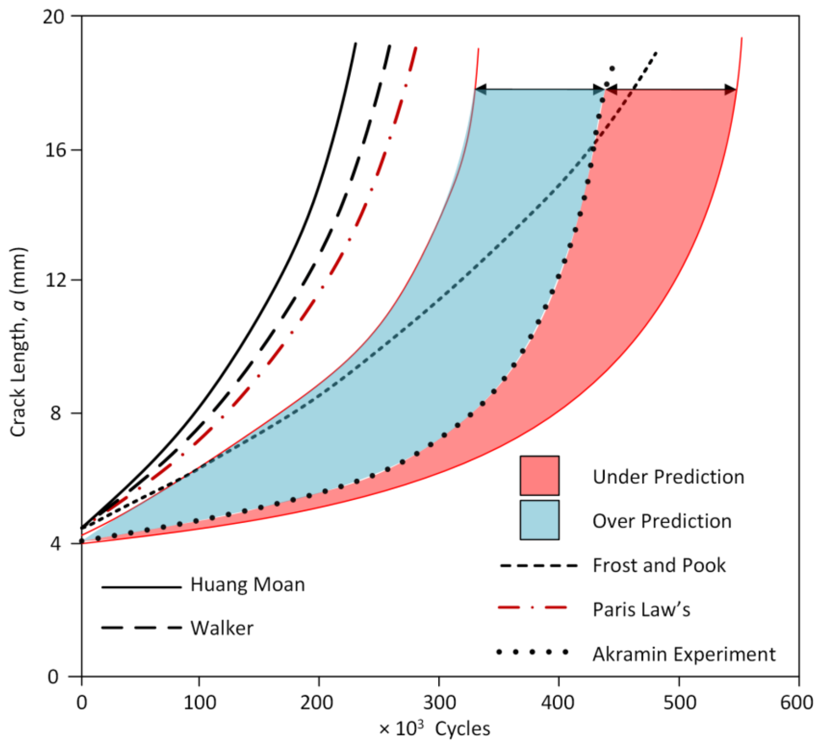

Figure 6. Schematic illustration of FCG models for fatigue life prediction.

Among the predictive models, the Huang-Moan model shows the fastest crack growth rate, significantly underestimating fatigue life by predicting failure at around 210×10^3cycles. Similarly, both Walker and Paris' Law models underestimate fatigue life, predicting failure earlier than the experimental data at approximately $240–270 \times 10^3$cycles. This indicates that both models are overly conservative for the current four-point bending configuration. In contrast, the Frost & Pook model best matches the experimental trend. It captures the gradual transition from stable to unstable crack growth more realistically and predicts fatigue failure at approximately $470–490 \times 10^3$cycles, which is slightly higher but much closer to the experimental fatigue life compared to the other models. Although minor deviations exist in the early crack growth stage, with slight overprediction, the overall trend alignment is satisfactory. Overall, the comparison indicates that the Frost & Pook model offers the most reliable prediction of fatigue crack growth behavior under four-point bending loading conditions, particularly in capturing the long stable crack-growth region before final rapid failure.

Fig. 6 illustrates the under- and over-life predictions based on the experimental outcome, which may lead to excessive risk-taking or maintenance costs. Excessive risk could lead to early failure, resulting in equipment and life loss. Because parts would need to be replaced too soon, excessive maintenance would shorten the life. As such, a precise forecast of the damage's actual response is necessary. Thus, fatigue-life forecasts based on FCG models can help avoid catastrophic failure. To achieve these aims, damage-life projections must be well defined.

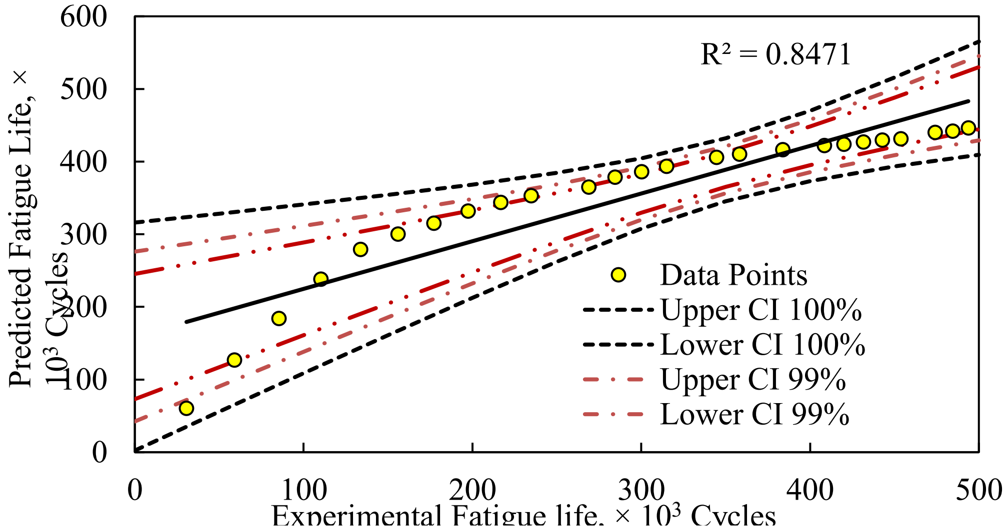

Figure 7. Frost & Pook fatigue crack growth model with regression line and confidence interval.

Fig. 7 and Fig. 8 show the correlation analysis of the fitted line plots of the Frost & Pook model and Paris Law model cycles against experimental cycles. The Walker and Huang Moan models were excluded from the graph because they ranked third and fourth in prediction performance, and because including them would clutter the graph. This technique was crucial in assessing fatigue life estimates that showed a higher degree of goodness of fit with the experimental data. The Paris law model shows a higher determination coefficient value, R^2 with 0.9076, against the Frost & Pook model, R^2 value of 0.8471. Thus, the Paris law model provides a better fit to the observations. Moreover, Fig. 7 and Fig. 8 show fatigue life predictions compared with experimental results, with 100%, 99%, and 95% confidence intervals within the life factor of 2 bands. The fatigue life prediction performs excellently compared with the experimental results within the 100% confidence interval. The predictions agree, as they fall within the 100% confidence interval. Most predictions fall within a life factor of two for the 95% confidence interval. The trend of the prediction interval among the two models is different. The Frost & Pook model trend is broader at the beginning and narrower in the middle, starting within the range of 200,000 to 400,000 cycles. Furthermore, the Frost & Pook model deviated from the experimental results [41] from 0 to 350,000 cycles, but after 350,000 cycles, it approached the experimental results. Meanwhile, the deviation of the Paris Law model is always constant across the number of experimental cycles, according to Fig. 8. Thus, the Frost & Pook model is considered to perform better because it converges more closely to the experimental data in the final stage of fatigue life, despite its lower R^2 value. In contrast, the Paris law model shows a relatively constant deviation across the overall fatigue life range.

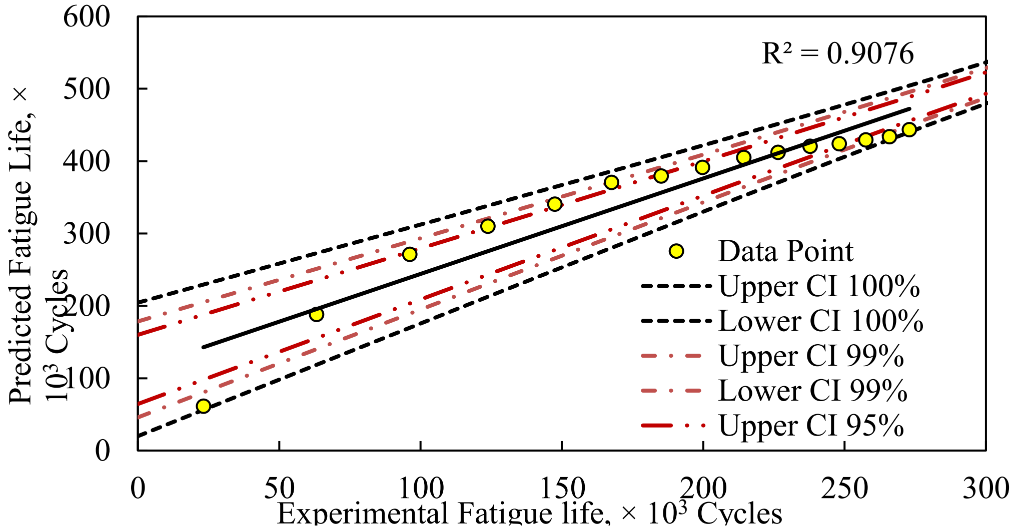

Figure 8. Paris Law fatigue crack growth model with regression line and confidence interval.

The prediction accuracy of the fatigue life models was evaluated using Mean Absolute Percentage Error (MAPE), Root Mean Square Error (RMSE), and Normalized Root Mean Square Error (NRMSE), as shown in Figs. 9, 10, and 11. These statistical indicators provide a comprehensive assessment of the deviation between predicted and experimental fatigue life results for the four-point bending configuration. From Fig. 11, the Frost and Pook model has the lowest NRMSE (0.1723), indicating the smallest normalized deviation from the experimental data among the models. In contrast, the Paris Law, Walker, and Huang Moan models show significantly higher NRMSE values of 0.4574, 0.5102, and 0.5759, respectively, demonstrating poorer predictive performance and larger deviations from the experimental trend.

A similar pattern is observed in Fig. 10, where the Frost and Pook model records the lowest RMSE value (65.85 × 10^3 cycles), whereas the Paris Law (174.77 × 10^3 cycles), Walker (194.94 × 10^3 cycles), and Huang Moan (220.06 × 10^3 cycles) models exhibit substantially higher error magnitudes. This indicates that the Frost and Pook formulation more accurately represents crack growth behavior under four-point bending loading conditions. Furthermore, Fig. 9 shows that the Frost and Pook model achieves the lowest MAPE value (16.87%), while the Paris Law, Walker, and Huang Moan models record higher errors of 50.64%, 55.93%, and 62.45%, respectively. Notably, all competing models exceed 50% error, whereas the Frost and Pook model remains below 20%, which is generally considered an acceptable range for engineering prediction accuracy. Overall, the combined error analysis confirms that the Frost and Pook model best agrees with experimental fatigue life data [41] under four-point bending conditions. Its consistently lower MAPE, RMSE, and NRMSE values indicate higher predictive reliability and better ability to capture fatigue crack growth behavior than the Paris Law, Walker, and Huang Moan models.

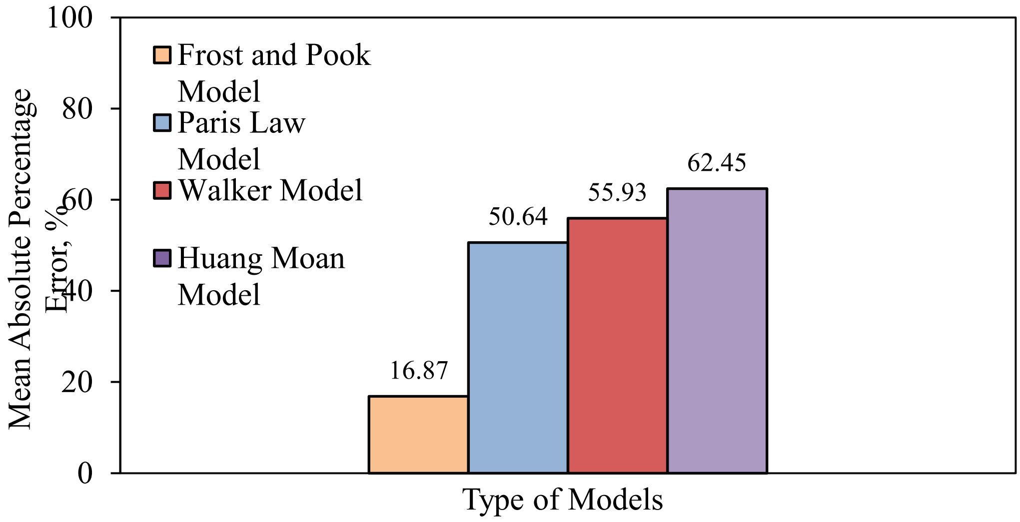

Figure 9. Bar chart of MAPE for fatigue life prediction.

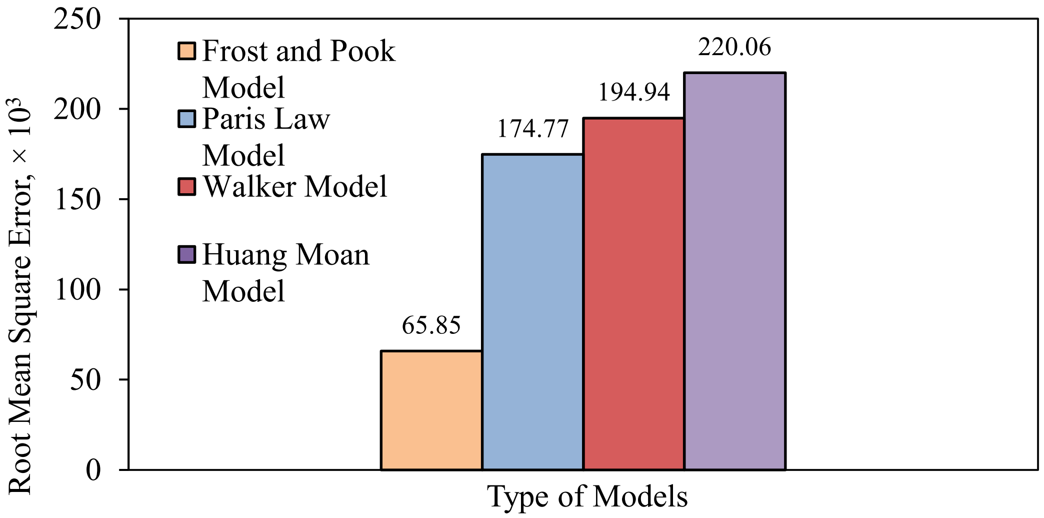

Figure 10. Bar chart of RMSE for fatigue life prediction.

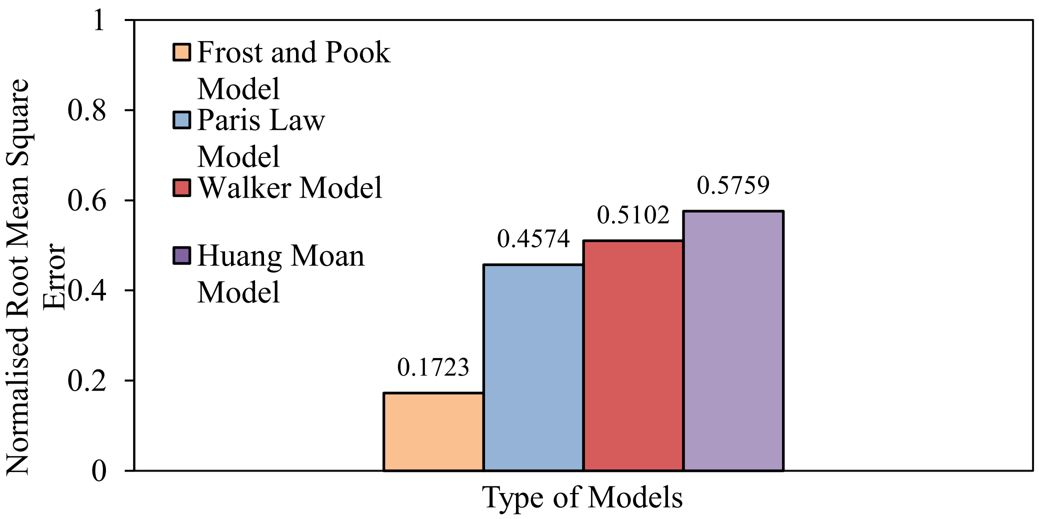

Figure 11. Bar chart of normalized RMSE for fatigue life prediction.

Although the Paris Law model exhibited a higher R^2 value in the correlation analysis, this indicator primarily reflects the overall linear relationship between the predicted and experimental fatigue lives rather than the prediction accuracy across the full fatigue crack growth life. Under four-point bending, the semi-elliptical surface crack did not propagate uniformly along the crack front. As the crack propagated, the remaining uncracked ligament became smaller, causing stresses near the crack front to redistribute and the crack growth rate to accelerate. Because the Paris Law model is based on a single power-law relationship, it shows a relatively constant deviation across the entire fatigue life range. In contrast, the Frost & Pook model captured the accelerated crack growth near the final stage of failure, which explains its closer agreement with the experimental fatigue life after approximately 300,000 cycles. This behavior is further supported by the lower RMSE, NRMSE, and MAPE values obtained for the Frost & Pook model, indicating superior predictive accuracy, particularly near failure.

4. CONCLUSIONS

Fatigue surface cracking is a principal cause of failure in metallic components and structures across various industries. Concerns about fatigue crack growth and structural reliability motivated this investigation into surface crack propagation under cyclic loading. From a practical engineering perspective, accurate fatigue life prediction supports damage-tolerant design and structural integrity management by enabling more reliable maintenance planning and reducing the risk of catastrophic failure. Four fatigue crack growth models Paris law, Frost and Pook, Walker, and Huang Moan were implemented in the fatigue crack analysis of a four-point bending specimen. The predicted fatigue lives were compared with experimental results to assess the performance of each model. The prediction accuracy was evaluated using the MAPE, RMSE, and NRMSE, as presented in Figs. 9–11. The results show that the Frost and Pook model provides the closest agreement with the experimental data [41], producing the lowest MAPE of 16.87%, RMSE of (65.85×10^3) cycles, and NRMSE of 0.1723. In comparison, the Paris law, Walker, and Huang Moan models produce substantially higher errors, with MAPE values exceeding 50% and NRMSE values ranging from 0.4574 to 0.5759. These results indicate lower predictive accuracy and greater deviation from the experimental fatigue life. Overall, the three error metrics consistently demonstrate that the Frost and Pook model provides the most accurate and reliable fatigue life prediction under the investigated four-point bending conditions. Its MAPE remains within the acceptable engineering error range of less than 20%, whereas the other models considerably overestimate the fatigue life. Therefore, fatigue life prediction using the Frost and Pook model may help prevent catastrophic failure by supporting appropriate inspection and maintenance intervals. The findings may also help prioritize critical components for monitoring and improve remaining useful life assessments for structural components subjected to cyclic bending loads.

ACKNOWLEDGEMENT

The authors would like to express their sincere gratitude to the Ministry of Higher Education, Malaysia, for their invaluable financial support through the Fundamental Research Grant Scheme (FRGS), Grant No. FRGS/1/2023/TK10/UMP/02/26 (RDU230134). Their support has been instrumental in the successful execution of this research project.

REFERENCES

[1] A. Grbović, G. Kastratović, A. Sedmak, I. Balać, and M. D. Popović, "Fatigue crack paths in light aircraft wing spars," *Int. J. Fatigue*, vol. 123, pp. 96–104, 2019, doi: https://doi.org/10.1016/j.ijfatigue.2019.02.013.

[2] M. Kikuchi, Y. Wada, and Y. Li, "Crack growth simulation in heterogeneous material by S-FEM and comparison with experiments," *Eng. Fract. Mech.*, vol. 167, pp. 239–247, 2016, doi: https://doi.org/10.1016/j.engfracmech.2016.03.038.

[3] M. Aursand, P. J. Haagensen, and B. H. Skallerud, "Remaining fatigue life assessment of corroded mooring chains using crack growth modelling," *Marine Structures*, vol. 90, p. 103446, 2023, doi: https://doi.org/10.1016/j.marstruc.2023.103446.

[4] H. Okada, H. Kawai, and K. Araki, "A virtual crack closure-integral method (VCCM) to compute the energy release rates and stress intensity factors based on quadratic tetrahedral finite elements," *Eng. Fract. Mech.*, vol. 75, no. 15, pp. 4466–4485, 2008, doi: https://doi.org/10.1016/j.engfracmech.2008.04.014.

[5] R. Masoudi Nejad and A. Gholami, "Fatigue crack growth and microstructural analysis of rail steel specimens under periodic overloads," *Mater. Today Commun.*, vol. 39, p. 108592, 2024, doi: https://doi.org/10.1016/j.mtcomm.2024.108592.

[6] T. Wang, Z. Bahrami, G. Renaud, C. Yang, M. Liao, and Z. Liu, "A probabilistic model for fatigue crack growth prediction based on closed-form solution," *Structures*, vol. 44, pp. 1583–1596, 2022, doi: https://doi.org/10.1016/j.istruc.2022.08.066.

[7] S. O. Afolabi, B. I. Oladapo, C. O. Ijagbemi, A. O. M. Adeoye, and J. F. Kayode, "Design and finite element analysis of a fatigue life prediction for safe and economical machine shaft," *Journal of Materials Research and Technology*, vol. 8, no. 1, pp. 105–111, 2019, doi: https://doi.org/10.1016/j.jmrt.2017.10.007.

[8] W. Liang, M. Lou, C. Zhang, D. Zhao, D. Yang, and Y. Wang, "Experimental investigation and phenomenological modeling of fatigue crack growth in X80 pipeline steel under random loading," *Int. J. Fatigue*, vol. 182, p. 108169, 2024, doi: https://doi.org/10.1016/j.ijfatigue.2024.108169.

[9] C. H. Wang and C. N. Duong, "Chapter 6 - Damage tolerance and fatigue durability of scarf joints," in *Bonded Joints and Repairs to Composite Airframe Structures*, C. H. Wang and C. N. Duong, Eds., Oxford: Academic Press, 2016, pp. 141–172. doi: https://doi.org/10.1016/B978-0-12-417153-4.00006-2.

[10] H. Zhang and P. Qiao, "Virtual crack closure technique in peridynamic theory," *Comput. Methods Appl. Mech. Eng.*, vol. 372, p. 113318, 2020, doi: https://doi.org/10.1016/j.cma.2020.113318.

[11] M. Goswami, S. Sharma, G. Subbarayan, S. P. A. Bordas, and S. Chattopadhyay, "Chapter Two - Historical purview and recent advances in fracture mechanics of elastomeric matrix composites," in *Advances in Applied Mechanics*, vol. 56, S. P. A. Bordas, Ed., Elsevier, 2023, pp. 139–187. doi: https://doi.org/10.1016/bs.aams.2022.09.002.

[12] B. Karihaloo and Q. Z. Xiao, "2.03 - Linear and Nonlinear Fracture Mechanics," in *Comprehensive Structural Integrity*, I. Milne, R. O. Ritchie, and B. Karihaloo, Eds., Oxford: Pergamon, 2003, pp. 81–212. doi: https://doi.org/10.1016/B0-08-043749-4/02128-5.

[13] H. Okada, H. Koya, H. Kawai, Y. Li, and K. Osakabe, "Computations of stress intensity factors for semi-elliptical cracks with high aspect ratios by using the tetrahedral finite element (fully automated parametric study)," *Eng. Fract. Mech.*, vol. 158, pp. 144–166, 2016, doi: https://doi.org/10.1016/j.engfracmech.2016.02.049.

[14] W. Xiang, M. Chen, Y. Tian, and B. Liu, "Application of a hierarchical quadrature element method to interface crack analysis in bi-material systems," *Eng. Fract. Mech.*, vol. 300, p. 109983, 2024, doi: https://doi.org/10.1016/j.engfracmech.2024.109983.

[15] P. Paris and F. Erdogan, "A critical analysis of crack propagation laws," 1963.

[16] O. E. Wheeler, "Spectrum loading and crack growth," 1972.

[17] R. G. Forman, "Study of fatigue crack initiation from flaws using fracture mechanics theory," *Eng. Fract. Mech.*, vol. 4, no. 2, pp. 333–345, 1972, doi: https://doi.org/10.1016/0013-7944(72)90048-3.

[18] K. Walker, "The effect of stress ratio during crack propagation and fatigue for 2024-T3 and 7075-T6 aluminum," 1970.

[19] N. E. Frost, L. P. Pook, and K. Denton, "A fracture mechanics analysis of fatigue crack growth data for various materials," *Eng. Fract. Mech.*, vol. 3, no. 2, pp. 109–126, 1971, doi: https://doi.org/10.1016/0013-7944(71)90003-8.

[20] T. Wang, Z. Bahrami, G. Renaud, C. Yang, M. Liao, and Z. Liu, "A probabilistic model for fatigue crack growth prediction based on closed-form solution," *Structures*, vol. 44, pp. 1583–1596, 2022, doi: https://doi.org/10.1016/j.istruc.2022.08.066.

[21] M. R. M. Akramin, M. S. Marizi, M. N. M. Husnain, and M. Shamil Shaari, "Analysis of Surface Crack using Various Crack Growth Models," *J. Phys. Conf. Ser.*, vol. 1529, no. 4, p. 042074, 2020, doi: 10.1088/1742-6596/1529/4/042074.

[22] W. J. Wang and M.-S. Yim, "A fatigue crack growth prediction model for cracked specimen under variable amplitude loading," *Int. J. Fatigue*, vol. 168, p. 107387, 2023, doi: https://doi.org/10.1016/j.ijfatigue.2022.107387.

[23] V. Ribeiro *et al.*, "Fatigue crack growth modelling by means of the strain energy density-based Huffman model considering the residual stress effect," *Eng. Fail. Anal.*, vol. 140, p. 106543, 2022, doi: https://doi.org/10.1016/j.engfailanal.2022.106543.

[24] N. Pugno, M. Ciavarella, P. Cornetti, and A. Carpinteri, "A generalized Paris' law for fatigue crack growth," *J. Mech. Phys. Solids*, vol. 54, no. 7, pp. 1333–1349, 2006, doi: https://doi.org/10.1016/j.jmps.2006.01.007.

[25] V. Ribeiro, J. Correia, G. Lesiuk, A. Gonçalves, A. De Jesus, and F. Berto, "Application and discussion of various crack closure models to predict fatigue crack growth in 6061-T651 aluminium alloy," *Int. J. Fatigue*, vol. 153, p. 106472, 2021, doi: https://doi.org/10.1016/j.ijfatigue.2021.106472.

[26] M. F. V Montezuma, E. P. De Deus, C. O. F. T. Rüchert, M. C. De Carvalho, and M. A. E Silva Filho, "Numerical-experimental procedure for predicting fatigue life in SAE AMS 7475-T7351 aluminum alloy considering the effect of stress ratio," *An. Acad. Bras. Cienc.*, vol. 96, 2024, doi: 10.1590/0001-3765202420231400.

[27] Y. Li, H. Wang, and D. Gong, "The interrelation of the parameters in the Paris equation of fatigue crack growth," *Eng. Fract. Mech.*, vol. 96, pp. 500–509, 2012, doi: 10.1016/j.engfracmech.2012.08.016.

[28] Y. Li and J. Jia, "A modified walker's equation in fatigue crack growth," *Xibei Gongye Daxue Xuebao/Journal of Northwestern Polytechnical University*, vol. 26, no. 2, pp. 221–224, 2008, [Online]. Available: https://www.scopus.com/inward/record.uri?eid=2-s2.0-44849123145&partnerID=40&md5=a11aa8b7e0638602de90c8576fa4c368

[29] P.-T. Guan, C.-Y. Lü, X.-T. Tang, J.-W. Zhu, Z.-Y. Ding, and Z.-L. Gao, "Study on fatigue crack growth behavior of q345r steel under multiple overloads," *Gongcheng Lixue/Engineering Mechanics*, vol. 34, no. 7, pp. 224-231and240, 2017, doi: 10.6052/j.issn.1000-4750.2016.02.0113.

[30] B. K. C. Yuen and F. Taheri, "Proposed modifications to the Wheeler retardation model for multiple overloading fatigue life prediction," *Int. J. Fatigue*, vol. 28, no. 12, pp. 1803–1819, 2006, doi: 10.1016/j.ijfatigue.2005.12.007.

[31] K. Tanaka, "4.04 - Fatigue Crack Propagation," in *Comprehensive Structural Integrity*, I. Milne, R. O. Ritchie, and B. Karihaloo, Eds., Oxford: Pergamon, 2003, pp. 95–127. doi: https://doi.org/10.1016/B0-08-043749-4/04089-1.

[32] M. Shaari, A. K. Ariffin, A. Takahashi, S. Abdullah, M. Kikuchi, and M. R. M. Akramin, “Fatigue crack growth analysis on square prismatic with embedded cracks under tension loading,” *JOURNAL OF MECHANICAL ENGINEERING AND SCIENCES*, vol. 14, pp. 2511–2525, Mar. 2017, doi: 10.15282/jmes.11.1.2017.10.0231.

[33] H. Okada, M. Higashi, M. Kikuchi, Y. Fukui, and N. Kumazawa, “Three dimensional virtual crack closure-integral method (VCCM) with skewed and non-symmetric mesh arrangement at the crack front,” *Eng. Fract. Mech.*, vol. 72, no. 11, pp. 1717–1737, 2005, doi: https://doi.org/10.1016/j.engfracmech.2004.12.005.

[34] D. Broek, *Elementary engineering fracture mechanics*. Springer Netherlands, 1982. [Online]. Available: https://books.google.com.my/books?id=LC4E7OjnhuEC

[35] G. Chell, “Developments in fracture mechanics,” 1979. [Online]. Available: https://api.semanticscholar.org/CorpusID:137575003

[36] M. Xinting, L. Guoxu, P. Jian, T. Ping, Z. Jinbo, and L. Jian, “Study on the I-II mixed mode fatigue crack growth behavior of TC4 titanium alloy,” *Theoretical and Applied Fracture Mechanics*, vol. 138, p. 104985, 2025, doi: https://doi.org/10.1016/j.tafmec.2025.104985.

[37] M.-S. Lee and M.-H. Kim, “A new fatigue crack growth model considering underloads and overloads history together with stress ratio,” *International Journal of Naval Architecture and Ocean Engineering*, vol. 14, p. 100481, 2022, doi: https://doi.org/10.1016/j.ijnaoe.2022.100481.

[38] J. Cong, Z. Liu, S. Zhou, S. Gao, and X. Zhu, “Predicting fatigue life and crack growth rate of TC4 titanium alloy based on PINN before and after ultrasonic impact treatment,” *Eng. Fail. Anal.*, vol. 166, p. 108875, 2024, doi: https://doi.org/10.1016/j.engfailanal.2024.108875.

[39] M. S. Shaari, M. R. M. Akramin, A. K. Ariffin, S. Abdullah, and M. Kikuchi, “Fatigue crack growth behaviour of semi-elliptical surface cracks for an API 5L X65 gas pipeline under tension,” *IOP Conf. Ser. Mater. Sci. Eng.*, vol. 308, no. 1, p. 012041, 2018, doi: 10.1088/1757-899X/308/1/012041.

[40] F. Y. Chin, M. S. Shaari, A. Takahashi, M. R. M. Akramin, and S. Urai, “Fatigue Crack Growth Behavior of AlSi10Mg Material Produced by Direct Metal Laser Sintering Using S-Version Finite Element Method,” *Journal of Failure Analysis and Prevention*, vol. 23, no. 2, pp. 601–608, 2023, doi: 10.1007/s11668-023-01643-6.

[41] M. R. M. Akramin, A. K. Ariffin, M. Kikuchi, and S. Abdullah, “Sampling method in probabilistic S-version finite element analysis for initial flaw size,” *Journal of the Brazilian Society of Mechanical Sciences and Engineering*, vol. 39, no. 1, pp. 357–365, 2017, doi: 10.1007/s40430-016-0549-z.